JACS
JOURNAL OF THE AMERICAN CHEMICAL SOCIETY
Article
pubs.acs.org/JACS

Metal–Metal Quadruple Bonds Supported by 5-Ethynylthiophene-2-carboxylato Ligands: Preparation, Molecular and Electronic Structures, Photoexcited State Dynamics, and Application as Molecular Synthons

Samantha E. Brown-Xu, Malcolm H. Chisholm,* Christopher B. Durr, and Thomas F. Spilker

Department of Chemistry and Biochemistry, The Ohio State University, Columbus, Ohio 43210, United States

Supporting Information

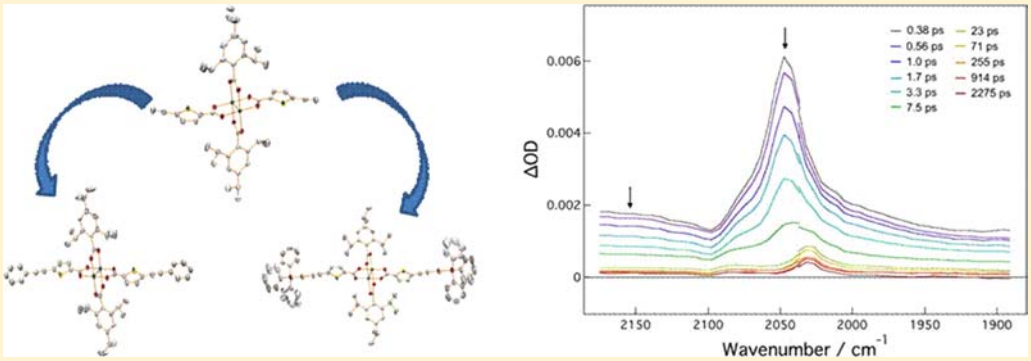

ABSTRACT: From the reaction between $M_2(T^iPB)_4$ and 2 equiv of 5-ethynylthiophene-2-carboxylic acid (H-ThCCH) in toluene, the complexes *trans*-$M_2(T^iPB)_2(ThCCH)_2$, where M = Mo (**I**) or W (**II**) and T^iPB = 2,4,6-triisopropyl benzoate, have been isolated and characterized by ^{1}H NMR, IR, MALDI-TOF MS, UV–vis, steady-state emission, transient absorption, and time-resolved infrared (TRIR) spectroscopies and single-crystal X-ray crystallography for **I**. The molecular structure of **I** confirms the *trans*-substitution pattern and the extended conjugation of the ethynylthienyl ligands via interaction with the $Mo_2\delta$ orbital. The HOMO of both **I** and **II** is the $M_2\delta$ orbital, and the intense color of the compounds (**I** is red and **II** is blue) is due to the $M_2\delta$-to-ThCCH ^{1}MLCT transition. The S_1 states for **I** and **II** are ^{1}MLCT. The T_1 state is ^{3}MLCT for **II**, but ^{3}MoMo$\delta\delta^*$ for **I**. The TRIR spectra of the ν(C≡C) stretch in the MLCT states are consistent with the delocalization of the electron over both ThCCH ligands. Compound **I** is shown to be a synthon for the preparation of *trans*-$Mo_2(T^iPB)_2(ThCCPh)_2$ (**III**) and *trans*-$Mo_2(T^iPB)_2(ThCCAuPPh_3)_2$ (**IV**). Both **III** and **IV** have been characterized spectroscopically and by single-crystal X-ray diffraction. The structure of **III** indicates the extended π-conjugation of the *trans*-ethynyl-thienyl units extends to the added phenyl rings.

1. INTRODUCTION

Conjugated organic polymers and even small oligomers are important in a range of rapidly emerging technologies including light-emitting diodes, field effect transistors, photovoltaic devices, and sensors.[1−6] The introduction of metal ions into these systems affords a variety of additional features, as is evident from fundamental studies by Hagihara[7] and the work of Wong in the introduction of platinum[8−14] and other metals[15,16] into conjugated ethynylthiophenes. The metal can enhance emission from triplet states by intersystem crossing and may allow hole transport by dπ–pπ conjugation.[17] We have for some time had an interest in the introduction of metal–metal (M_2) quadruply bonded units into organic π-systems and in the preparation of metalated polymers. The $M_2\delta$ orbital can interact directly with a π-conjugated organic molecule that is attached to the M_2 unit via a carboxylate or the related amidinate ligand.[18−23] We have previously attempted to prepare polymers/oligomers containing M_2 units by the reaction between the homoleptic carboxylates $M_2(O_2CR)_4$ and conjugated dicarboxylic acids. For M = Mo and ter- and pentathienyl (α,α'-linked) dicarboxylic acids, oligomers were obtained suitable for spin coating and, when fabricated, showed electroluminescence.[24] However, this procedure gave only low-molecular-weight materials having 6–8 M_2 units and containing molecular loops, triangles, and other species. Indeed, reactions involving the smallest of dicarboxylic acids, namely oxalic acid, gave almost exclusively triangles.[25] We are therefore seeking alternate strategies for the synthesis of oligomers and polymers by employing ethynyl and vinyl end groups that may be used in more well-developed carbon–carbon coupling reactions and eliminate the reliance on metathetic reactions at the M_2 center.

Received: January 16, 2013
Published: May 24, 2013

   dx.doi.org/10.1021/ja400508u | *J. Am. Chem. Soc.* 2013, 135, 8254–8259

Scheme 1. Synthesis of I–IV[a]

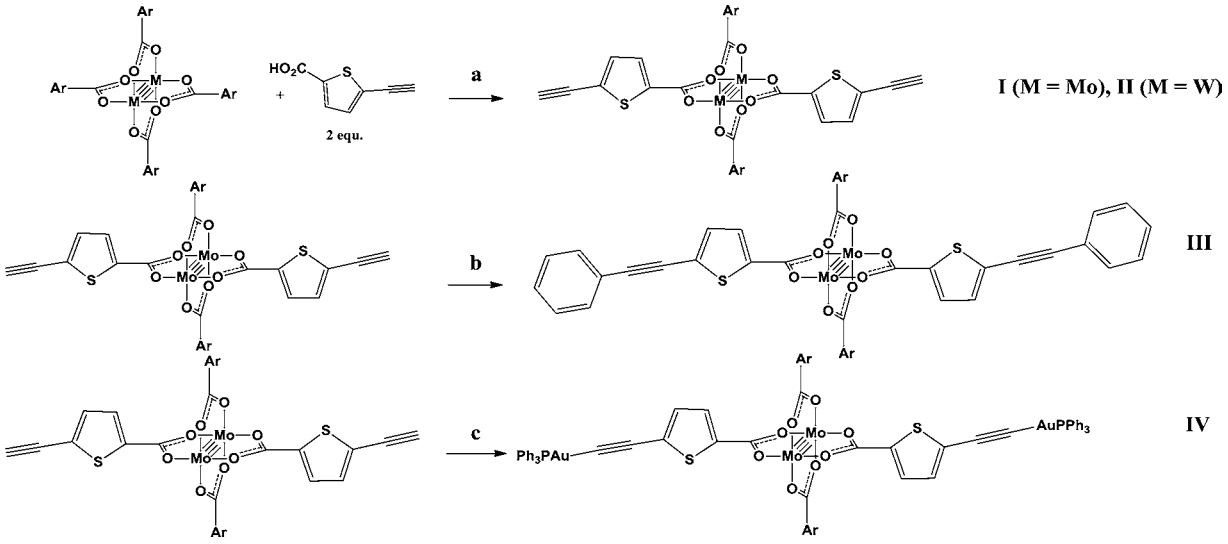

[a]Ar = 2,4,6-triisopropylphenyl. Reagents: (a) toluene, (b) excess phenyl iodide, THF:Et_3N, $Pd(PPh_3)_2Cl_2$, CuI; (c) 2 equiv of Ph_3PAuCl, Et_3N, THF:DCM.

We describe here the synthesis of thienylcarboxylates bearing terminal ethynyl groups bound to the M_2 center and show that these are viable synthons for the synthesis of extended π-systems and molecular triads. The two principal quadruply bonded complexes are also shown to exhibit very interesting photophysical properties.

2. RESULTS AND DISCUSSION

2.1. Preparation. The synthesis of the new compounds reported in this work is outlined in Scheme 1.

The compounds *trans*-$Mo_2(T^iPB)_2(ThCCH)_2$, where M = Mo (**I**) and W (**II**), T^iPB = 2,4,6-triisopropyl benzoate, and ThCCH = 5-ethynylthiophene-2-carboxylate, are soluble in toluene, THF, and dichloromethane (DCM). They are air-sensitive and intensely colored: **I** is red, and **II** is blue. They give molecular ions in the MALDI-TOF MS, and their ^1H NMR and other characterization data are given in the Supporting Information.

The compound *trans*-$Mo_2(T^iPB)_2(ThCCPh)_2$ (**III**) was prepared by Sonogashira coupling involving phenyl iodide. Compound **III** is purple, in contrast to its precursor **I**. The gold-containing complex, *trans*-$Mo_2(T^iPB)_2(ThCCAuPPh_3)_2$ (**IV**), is red like its precursor **I**. Further characterization data for **III** and **IV** are given in the Supporting Information.

2.2. Single-Crystal and Molecular Structures. The molecular structures of the dimolybdenum-containing complexes **I**, **III**, and **IV** are shown in Figures 1, 2, and 3, respectively.

Each structure has a molecular center of inversion, and the phenyl rings of the T^iPB ligands are essentially out of conjugation with the carboxylate π-system. The dihedral planes involving the CO_2 and C_6 rings are 86.7° (**I**), 85.2° (**III**), and 81.9° (**IV**). In contrast, the thienyl ring and its attendant carboxylate are nearly planar, with dihedral angles of 3.8° (**I**), 7.7° (**III**), and 1.4° (**IV**). For compound **III**, the dihedral angle between the phenyl and thienyl rings is 9.3°. The central $Mo_2(O_2R)_4$ units are typical of Mo_2^{4+} quadruply bonded complexes, with Mo–Mo and Mo–O bond distances of ~2.10 Å.[26] All three compounds crystallized with donor solvent molecules, THF (**I** and **III**) and DMF (**IV**), along the Mo–Mo axis.

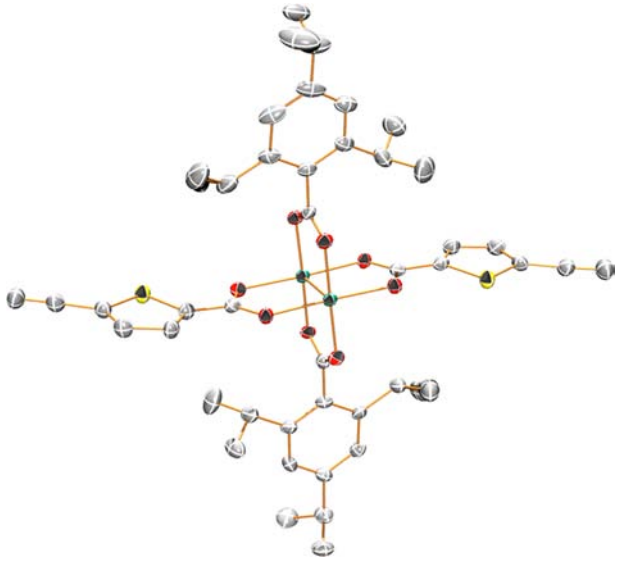

Figure 1. Thermal ellipsoid plot of **I** shown at 50% probability. Hydrogens and solvent molecules have been omitted for clarity. Color code: gray, carbon; blue, nitrogen; scarlet, oxygen; yellow, sulfur; green, molybdenum.

Further crystallographic details can be found in the Supporting Information.

2.3. Electronic Structure Calculations. In order to aid in the interpretation of the spectral data, we performed electronic structure calculations on the model compounds **I′**, **II′**, and **III′**, where formate is substituted for the T^iPB ligands. This assists in reducing the computational time and resources and has proven useful for related compounds and interpretation of their spectral data. The calculations employed Density Functional Theory (DFT) and time-dependent DFT (TD-DFT). We also performed calculations on the anions $[\mathbf{I'}]^-$ and $[\mathbf{II'}]^-$ to assist in the determination of electron delocalization in the MLCT states.

dx.doi.org/10.1021/ja400508u | J. Am. Chem. Soc. 2013, 135, 8254–8259

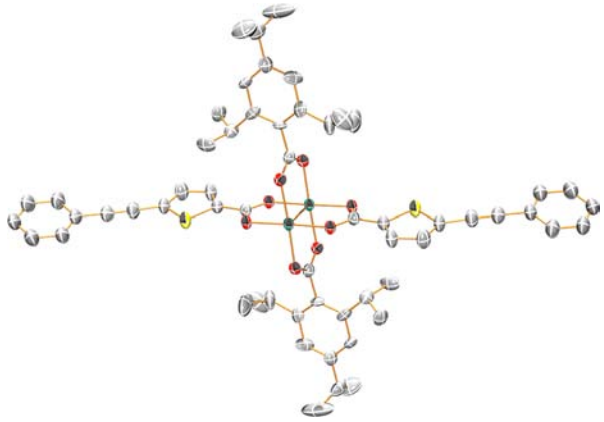

Figure 2. Thermal ellipsoid plot of **III** shown at 50% probability. Hydrogens and solvent molecules have been omitted for clarity. Color code: gray, carbon; blue, nitrogen; scarlet, oxygen; yellow, sulfur; green, molybdenum.

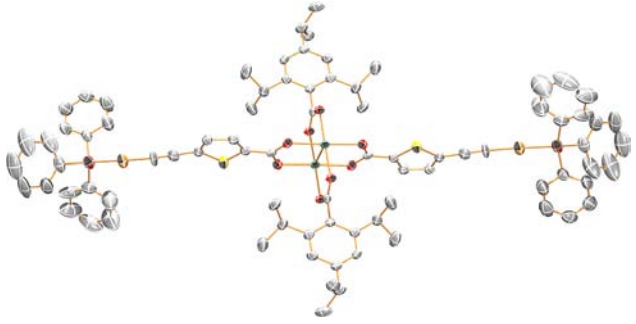

Figure 3. Thermal ellipsoid plot of **IV** shown at 50% probability. Hydrogens and solvent molecules have been omitted for clarity. Color code: gray, carbon; blue, nitrogen; scarlet, oxygen; yellow, sulfur; maroon, phosphorus; orange, gold; green, molybdenum.

Figure 4 displays the frontier molecular orbital energy level diagram comparing **I′** and **II′** and isosurface contour plots for **II′**, which are very similar to those for **I′**. For each molecule, the highest occupied molecular orbital (HOMO) is $M_2\delta$ with a significant degree of mixing with the ligands. The lowest unoccupied molecular orbital (LUMO) in both cases is the symmetrical combination of the ethynylthienyl carboxylate π^* orbital that cannot mix with the $M_2\delta$. For molybdenum, the HOMO−1 and HOMO−2 are filled combinations of the ethynylthienyl carboxylate, which lie higher in energy relative to the $M_2\pi$ and $M_2\sigma$ orbitals. In the case of tungsten, the order of the ligand and metal π orbitals is reversed as the metal-based orbitals, δ and π for tungsten, lie roughly 0.5 eV higher relative to their molybdenum counterparts. For molybdenum, the LUMO+1 is the $Mo_2\delta^*$ orbital, and the LUMO+2 is the ligand-based π^* orbital of the ethynylthienyl carboxylate that mixes with the $M_2\delta$. For tungsten, $M_2\delta^*$ is the LUMO+2, and it is well separated from the ligand π^* combinations, the LUMO and LUMO+1. The HOMO−LUMO gap for tungsten is also 0.5 eV smaller than that of its molybdenum analogue.

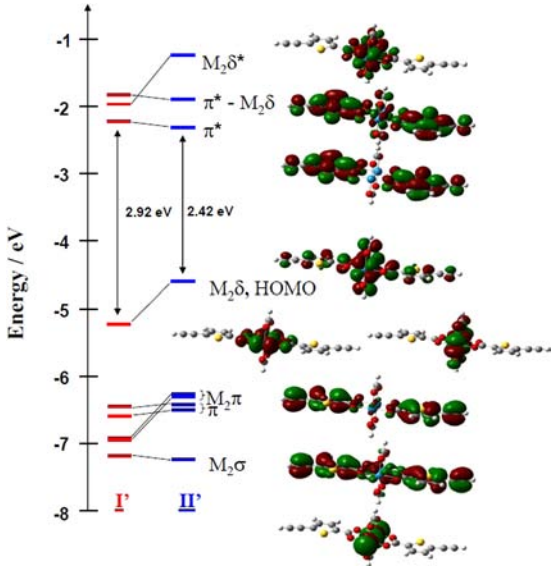

Figure 4. Energy diagram of compounds **I′** and **II′**. Orbitals for **II′** were generated with Gaussview 5.0.

A similar comparison of the frontier orbitals of **I′** and **III′** along with the isosurface contour plots of **III′** are shown in Figure 5. The calculations for both **I′** and **III′** were done in C_{2h} symmetry, which emphasizes the maximum ligand π−$M_2\delta$ conjugation. For **III′** we see a greater mixing of the ligand filled π orbitals with the $M_2\delta$ as a result of the higher energy of the ligand filled π orbitals in **III′** relative to **I′**. This has the effect of raising the energy of the HOMO, while the LUMO in **III′** is lowered due to the extended π conjugation. The energy separation between the LUMO and LUMO+2 orbitals, representing the two ligand π^* systems, is also greater for **III′**, 0.33 versus 0.26 eV, as a result of the greater $M_2\delta$ ligand π orbital mixing.

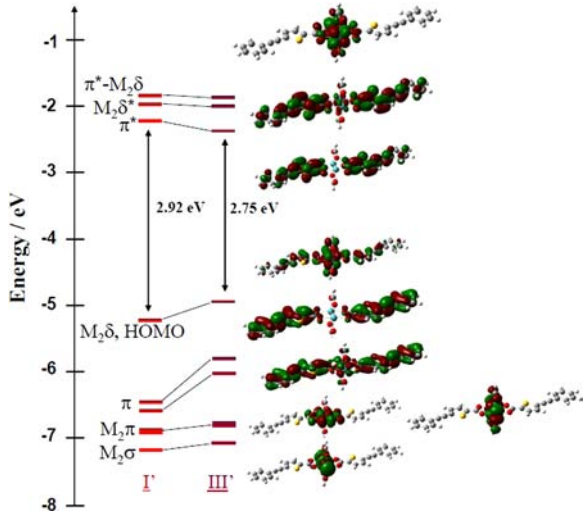

Figure 5. Energy diagram for **I′** and **III′**. Orbitals for **III′** are shown.

2.4. Electronic Absorption Spectra. The UV−vis−NIR spectra of compounds **I** and **II** in THF at room temperature are compared in Figure 6. At high energy, ∼300 nm, we see the ethynylthienyl carboxylate ligand-based π−π^* transition that is hardly influenced by the metal. In contrast, to lower energy we see the intense ^{1}MLCT (metal-to-ligand charge-transfer) bands arising from the $M_2\delta$ to ethynylthienyl carboxylate π^*, HOMO→LUMO, that track with the relative energy of the $M_2\delta$ orbital. We also see evidence of a vibronic progression in the spectrum of **II** for which the (0,0) transition is the most intense. The vibronic features appear better resolved at low temperature in 2-MeTHF, and the spectrum at 125 K is shown

dx.doi.org/10.1021/ja400508u | J. Am. Chem. Soc. 2013, 135, 8254−8259

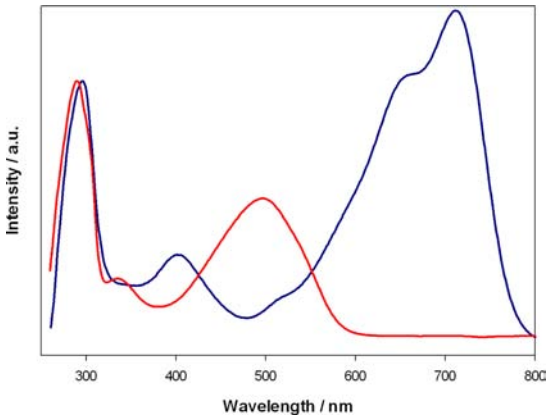

Figure 6. Electronic absorption spectra for **I** (red) and **II** (blue). MLCT λ_{max} = 499 (**I**) and 712 nm (**II**).

in the Supporting Information. This feature is common to many tungsten complexes of this type and has been discussed elsewhere.[27−29] Also, for both compounds we see the $M_2\delta$-to-$CO_2\pi^*$ transition associated with the T^{t}PB ligand: 402 nm for M = W and 335 nm for M = Mo.

An analogous comparison of the absorption spectra of the Mo_2-containing compounds, **I**, **III**, and **IV**, is given in Figure 7.

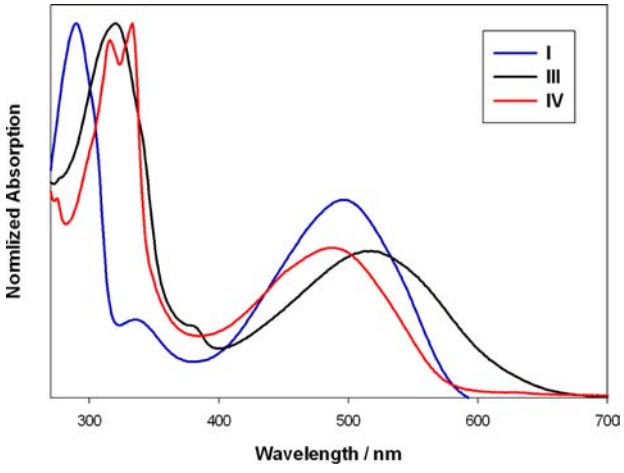

Figure 7. Electronic absorption spectra of **I**, **III**, and **IV** in THF at room temperature. MLCT λ_{max} = 499 (**I**), 517 (**III**), and 489 nm (**IV**).

Here we see the similarity of compounds **I** and **IV**, which both appear red. This is not too surprising since the $[AuPPh_3]^+$ cation is commonly referred to as a "large proton".[30] In contrast, the ^{1}MLCT of compound **III** is notably red-shifted to lower energy compared to **I** as a result of the extended π system. The intraligand $\pi\rightarrow\pi^*$ transition in **III** (321 nm) also occurs at lower energy than in **I** (290 nm).

2.5. Solvent Dependence and Steady-State Emission. The absorption and steady-state emission spectra associated with the ^{1}MLCT states have been recorded in THF, toluene, and DCM at room temperature. These are shown for **I** and **II** in Figure 8, where it can be seen that while there is a significant solvent dependence in the absorption spectra, there is very little in the emission from the S_1 state between toluene and DCM, but in the case of THF we do see a significant shift, which is not surprising because THF can behave as a good ligand in axial coordination to the M_2^{5+} center in the MLCT state. This essentially stabilizes the MLCT state in THF. The emission of

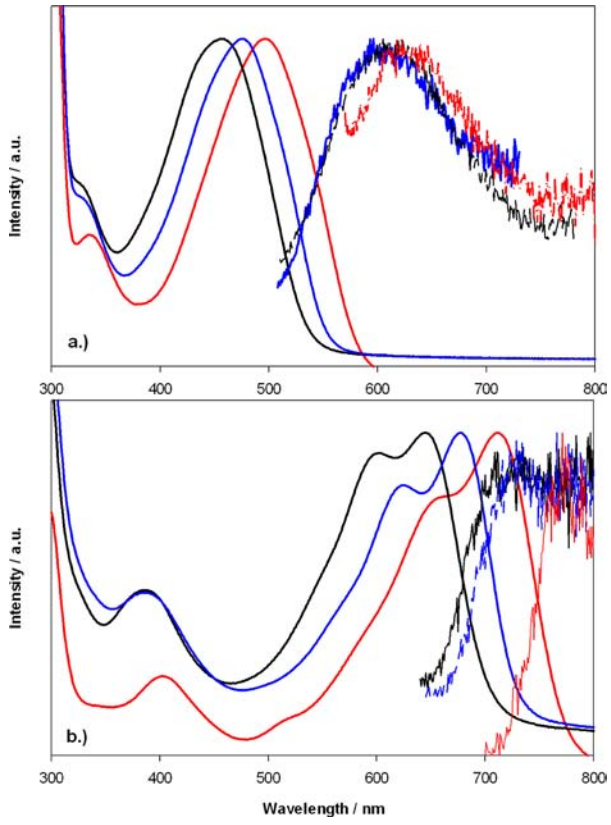

Figure 8. Solvent-dependent absorption and emission spectra of **I** (a) and **II** (b) in THF (red), DCM (black), and toluene (blue).

II in toluene was measured as a function of concentration and displays no shift in the spectrum, ruling out any self-absorption (SI Figure 1).

At room temperature, the absorption spectra correspond to a Boltzmann distribution of rotamers along the ethynylthienyl carboxylate, and both *trans*-ligands are relatively weakly coupled. However, upon photoexcitation, the promoted electron formally occupies the LUMO, which has a stronger preference for extended planarity. Thus, photoexcitation may well be expected to lead to an initially polar excited state that relaxes to one that is nonpolar. The steady-state emission spectra support this view that the S_1 state has little if any dipole moment. Alternately stated, S_1 is a delocalized excited state with the positive charge on the M_2 center and the electron delocalized over both ethynylthienyl carboxylate ligands. This view is further supported by the TRIR spectra, *vide infra*.

We have not determined the quantum yield for the emission, but it is akin to other dimetal tetracarboxylates for which the efficiency was estimated to be less than 0.1%.[31]

Compound **I** also shows phosphorescence from its triplet (T_1) state at ∼1100 nm which is typical of Mo_2-containing carboxylates and corresponds to a ^{3}MoMo$\delta\delta^*$ state (SI Figure 2).[18,20−22,32] At 77 K, the emission intensity increases notably on cooling, and a vibronic progression corresponding to the Mo−Mo stretch (∼350 cm^{-1}) is visible. Compound **II** has singlet (S_1) emission with $\lambda_{max} \approx$ 870 nm, which is followed by tailing to ∼1100 nm. There is a definite weak emission at 1260 nm which we suggest arises from weak phosphorescence from the ^{3}MLCT state at room temperature (SI Figure 2). We have seen this type of behavior previously for tungsten, and it leads to ∼3500 cm^{-1} in terms of the energy separation of the S_1 and

dx.doi.org/10.1021/ja400508u | J. Am. Chem. Soc. 2013, 135, 8254−8259

T_1 MLCT states (SI Figure 2, inset).[33] It should be noted that the ^{3}WW $\delta\delta^*$ state is notably higher in energy than the ^{3}MoMo $\delta\delta^*$ state because of the relative energies of the $M_2\delta$ orbitals. This is nicely seen in the absorption spectra of $M_2(T^iPB)_4$ compounds, where the λ_{max} occurs at longer wavelength for $M_2 = W_2$, whereas the phosphorescence is in the inverse order.[32]

2.6. Time-Resolved Spectroscopy. Compounds **I** and **II** have been examined by femtosecond time-resolved infrared (fs-TRIR) and nanosecond transient absorption (ns-TA) spectroscopies. From these we can estimate the S_1 lifetimes as 3.57 ps for **I** and 4.4 ps for **II** (SI Figure 3), while the T_1 lifetimes are 78.8 ± 5.9 μs for **I** and 10−30 ns for **II** (SI Figure 4). Most pertinent to the matter of charge location in the excited states are the TRIR spectra associated with the ethynyl group. In the ground state, this is a weak IR-active stretch seen at ν = 2099 cm^{-1} for both compounds. Upon photoexcitation, the vibration has enhanced intensity and is shifted to lower energy due to population of the π^* orbital. For complex **II** (Figure 9), the IR

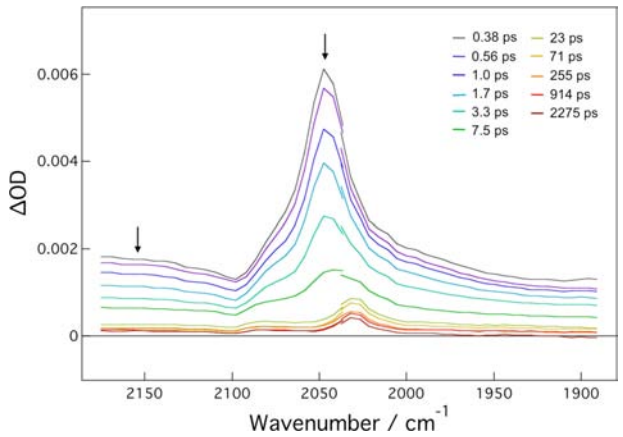

Figure 9. fs-TRIR of ν(C≡C) of **II** in THF at room temperature, λ_{ex} = 720 nm.

band assignable to ν(C≡C) is initially shifted by 52 cm^{-1} in the ^{1}MLCT state. This peak decays with time to leave an IR band assignable to the ^{3}MLCT state of **II** shifted 68 cm^{-1} to lower energy. The appearance of a single IR-active mode is consistent with a delocalized excited state and contrasts with the spectra of compounds of the form *trans*-$PtL_2((C{\equiv}CAr)_2$ that show two IR stretches in their T_1 states: one shifted to lower energy and the other to higher energy relative to the ground state.[34,35] These have been ascribed to broken or C_{2v} symmetry in the excited state. The further shift of the ν(C≡C) to lower energy in **II** with the change from S_1 to T_1 suggests that there is slightly greater C≡C π^* character in the triplet state. The molybdenum complex **I** (SI Figure 5) shows similar behavior, with $\Delta\nu$(C≡C) = −66 cm^{-1} in the S_1 state. Following decay to the T_1 state, however, the ethynyl stretch becomes IR silent, consistent with a ^{3}MoMo$\delta\delta^*$ state.

Since the IR bands associated with ligands in MLCT states are very similar to those of the reduced form of the ligand, we have calculated the values of ν(C≡C) for $[\mathbf{I}']^-$ and $[\mathbf{II}']^-$. The calculations pertain to a delocalized anion with the negative charge distributed principally upon the two *trans*-ethynylthienyl carboxylates. A comparison of the experimental values for compounds **I** and **II** in their ground and photoexcited states is given in Table 1, along with those calculated for the ground states of **I′** and **II′** and their respective anions $[\mathbf{I}']^-$ and $[\mathbf{II}']^-$. The calculated shifts for the anions (~55 cm^{-1}) compare

Table 1. Experimental and Computational ν(CC) Frequencies (in cm^{-1}) and Corresponding Shifts for I and II

	I	II		I′	II′
S_0	2099	2099	neutral	2130	2128
S_1 (T_1)	2033	2047 (2031)	anion	2073	2073
$\Delta\nu$(CC)	−66	−52 (−68)	$\Delta\nu$(CC)	−57	−55

favorably with those observed in the S_1 states, supporting the view of a delocalized excited state.[36]

Time-resolved spectroscopic studies of **III** and **IV** will be reported later in conjunction with other compounds of similar nature. Evaluating the shift of ν(C≡C) in comparison to the parent complexes should provide a measure of the electronic interaction of their appended groups in the excited states.

3. CONCLUDING REMARKS

The spectroscopic data for compounds **I** and **II** indicate that the S_1 states and the T_1 state for **II** are fully delocalized. In terms of excited-state mixed valency,[37] this is Class III on the Robin and Day scheme.[38] There are, to our knowledge, no detailed TRIR studies of transition metal alkynyl complexes in their S_1 states, despite the fact that some fluoresce and have picosecond lifetimes. The T_1 states that have been examined have broken symmetry where the charge is centered upon one ligand. The delocalized ^{3}MLCT states of **II** thus appear very different from all studies of *trans*-bisalkynyl Pt(II) complexes to date, which show lowest energy electronic transitions that are at least in part MLCT in character.[39−47]

In terms of the synthetic strategy for the synthesis of higher order assemblies, the preparation of **III** and **IV** from **I** is very encouraging. Although the C−C coupling reactions employed are "standard" in organic synthesis, and have been successfully employed by others in the synthesis of later transition metal-containing organic conjugated oligomers and polymers,[48−54] the application to the kinetically labile M_2^{4+} center is notable, as many reactions may lead to undesired products due to metathetic reactions of the carboxylates. For example, the use of organomagnesium or organozinc reagents as in Kumada or Negishi coupling reactions is not possible due to carboxylate scrambling. Further work involving C−C coupling reactions of this type involving vinyl groups is currently underway.

■ ASSOCIATED CONTENT

Supporting Information

Materials and methods, synthesis and characterization of **I**−**IV**, NIR emission spectra, kinetic traces of **I** and **II** from the fs-TRIR and of **I** from the ns-TA, TRIR spectrum of **I**, and crystallographic information (CIF). This material is available free of charge via the Internet at http://pubs.acs.org. CCDC records 919547−919549 contain the supplementary crystallographic data for this paper. These data can be obtained free of charge from The Cambridge Crystallographic Data Centre via www.ccdc.cam.ac.uk/data_request/cif.

■ AUTHOR INFORMATION

Corresponding Author

chisholm@chemistry.ohio-state.edu

Notes

The authors declare no competing financial interest.

■ ACKNOWLEDGMENTS

The authors acknowledge Dr. Judith Gallucci for helpful discussion and Prof. Claudia Turro for use of instrumentation. This work was supported by NSF grant CHE-0957191 and the OSU Institute for Materials Research. Computational resources were provided by the Ohio Supercomputing Center. S.E.B.-X. acknowledges support from the National Defense Science and Engineering Graduate (NDSEG) Fellowship. During this work we discovered that compound **I** has been prepared and structurally characterized independently by Thomas P. Robinson in the group of Prof. Paul R. Raithby in the University of Bath, UK.

■ REFERENCES

(1) Mishra, A.; Bäuerle, P. *Angew. Chem., Int. Ed.* **2012**, *51*, 2020−2067.
(2) Osaka, I.; Shimawaki, M.; Mori, H.; Doi, I.; Miyazaki, E.; Koganezawa, T.; Takimiya, K. *J. Am. Chem. Soc.* **2012**, *134*, 3498−3507.
(3) Silvestri, F.; Marrocchi, A.; Seri, M.; Kim, C.; Marks, T. J.; Facchetti, A.; Taticchi, A. *J. Am. Chem. Soc.* **2010**, *132*, 6108−6123.
(4) McCulloch, I.; Ashraf, R. S.; Biniek, L.; Bronstein, H.; Combe, C.; Donaghey, J. E.; James, D. I.; Nielsen, C. B.; Schroeder, B. C.; Zhang, W. *Acc. Chem. Res.* **2012**, *45*, 714−722.
(5) Bronstein, H.; Chen, Z.; Ashraf, R. S.; Zhang, W.; Du, J.; Durrant, J. R.; Shakya Tuladhar, P.; Song, K.; Watkins, S. E.; Geerts, Y.; Wienk, M. M.; Janssen, R. A. J.; Anthopoulos, T.; Sirringhaus, H.; Heeney, M.; McCulloch, I. *J. Am. Chem. Soc.* **2011**, *133*, 3272−3275.
(6) Tsao, H. N.; Cho, D.; Andreasen, J. W.; Rouhanipour, A.; Breiby, D. W.; Pisula, W.; Müllen, K. *Adv. Mater.* **2009**, *21*, 209−212.
(7) Sonogashira, K.; Takahashi, S.; Hagihara, N. *Macromolecules* **1977**, *10*, 879−880.
(8) Wong, W.-Y.; Wang, X.-Z.; He, Z.; Chan, K.-K.; Djurišić, A. B.; Cheung, K.-Y.; Yip, C.-T.; Ng, A. M.-C.; Xi, Y. Y.; Mak, C. S. K.; Chan, W.-K. *J. Am. Chem. Soc.* **2007**, *129*, 14372−14380.
(9) Zhan, H.; Wong, W.-Y.; Ng, A.; Djurišić, A. B.; Chan, W.-K. *J. Organomet. Chem.* **2011**, *696*, 4112−4120.
(10) Wong, W.-Y.; Ho, C.-L. *Acc. Chem. Res.* **2010**, *43*, 1246−1256.
(11) Wong, W.-Y. *Macromol. Chem. Phys.* **2008**, *209*, 14−24.
(12) Ho, C.-L.; Wong, W.-Y. *Coord. Chem. Rev.* **2011**, *255*, 2469−2502.
(13) Wong, W.-Y.; Wang, X.-Z.; He, Z.; Djurišić, A. B.; Yip, C.-T.; Cheung, K.-Y.; Wang, H.; Mak, C. S. K.; Chan, W.-K. *Nat. Mater.* **2007**, *6*, 521−527.
(14) Wong, W.-Y.; Ho, C.-L. *Coord. Chem. Rev.* **2006**, *250*, 2627−2690.
(15) Li, P.; Ahrens, B.; Choi, K.-H.; Khan, M. S.; Raithby, P. R.; Wilson, P. J.; Wong, W.-Y. *CrystEngComm* **2002**, *4*, 405−412.
(16) Wong, W.-Y.; Choi, K.-H.; Lu, G.-L.; Lin, Z. *Organometallics* **2002**, *21*, 4475−4481.
(17) Holliday, B. J.; Swager, T. M. *Chem. Commun.* **2005**, 23−36.
(18) Burdzinski, G. T.; Chisholm, M. H.; Chou, P.-T.; Chou, Y.-H.; Feil, F.; Gallucci, J. C.; Ghosh, Y.; Gustafson, T. L.; Ho, M.-L.; Liu, Y.; Ramnauth, R.; Turro, C. *Proc. Natl. Acad. Sci. U.S.A.* **2008**, *105*, 15247−15252.
(19) Chisholm, M. H.; D'Acchioli, J. S.; Hadad, C. M. *J. Cluster Sci.* **2006**, *18*, 27−49.
(20) Alberding, B. G.; Chisholm, M. H.; Ghosh, Y.; Gustafson, T. L.; Liu, Y.; Turro, C. *Inorg. Chem.* **2009**, *48*, 8536−8543.
(21) Brown-Xu, S. E.; Chisholm, M. H.; Gallucci, J. C.; Ghosh, Y.; Gustafson, T. L.; Reed, C. R. *Dalton Trans.* **2012**, *41*, 2257−2263.
(22) Brown-Xu, S. E.; Chisholm, M. H.; Durr, C. B.; Gustafson, T. L.; Naseri, V.; Spilker, T. F. *J. Am. Chem. Soc.* **2012**, *134*, 20820−20826.
(23) Chisholm, M. H.; Patmore, N. J. *Acc. Chem. Res.* **2007**, *40*, 19−27.
(24) Chisholm, M. H.; Epstein, A. J.; Gallucci, J. C.; Feil, F.; Pirkle, W. *Angew. Chem., Int. Ed.* **2005**, *44*, 6537−6540.
(25) Chisholm, M. H.; Durr, C. B.; Hadad, C. M.; Spilker, T. F. *J. Cluster Sci.* **2012**, *23*, 767−780.
(26) Cotton, F. A.; Murillo, C. A.; Walton, R. A. *Multiple Bonds Between Metal Atoms*, 3rd ed.; Springer Science and Business Media, Inc.: New York, 2005.
(27) Bursten, B. E.; Chisholm, M. H.; Clark, R. J. H.; Firth, S.; Hadad, C. M.; MacIntosh, A. M.; Wilson, P. J.; Woodward, P. M.; Zaleski, J. M. *J. Am. Chem. Soc.* **2002**, *124*, 3050−3063.
(28) Alberding, B. G.; Chisholm, M. H.; Lear, B. J.; Naseri, V.; Reed, C. R. *Dalton Trans.* **2011**, *40*, 10658−10663.
(29) Chisholm, M. H.; Lear, B. J. *Chem. Soc. Rev.* **2011**, *40*, 5254−5265.
(30) Raubenheimer, H. G.; Schmidbaur, H. *Organometallics* **2012**, *31*, 2507−2522.
(31) Chisholm, M. H.; Gustafson, T. L.; Turro, C. *Acc. Chem. Res.* **2013**, *46*, 529−538.
(32) Alberding, B. G.; Chisholm, M. H.; Chou, Y.-H.; Gallucci, J. C.; Ghosh, Y.; Gustafson, T. L.; Patmore, N. J.; Reed, C. R.; Turro, C. *Inorg. Chem.* **2009**, *48*, 4394−4399.
(33) Chisholm, M. H.; Chou, P.-T.; Chou, Y.-H.; Ghosh, Y.; Gustafson, T. L.; Ho, M.-L. *Inorg. Chem.* **2008**, *47*, 3415−3425.
(34) Emmert, L. A.; Choi, W.; Marshall, J. A.; Yang, J.; Meyer, L. A.; Brozik, J. A. *J. Phys. Chem. A* **2003**, *107*, 11340−11346.
(35) Batista, E. R.; Martin, R. L. *J. Phys. Chem. A* **2005**, *109*, 9856−9859.
(36) Alberding, B. G.; Chisholm, M. H.; Gallucci, J. C.; Ghosh, Y.; Gustafson, T. L. *Proc. Natl. Acad. Sci. U.S.A.* **2011**, *108*, 8152−8156.
(37) Plummer, E. A.; Zink, J. I. *Inorg. Chem.* **2006**, *45*, 6556−6558.
(38) Robin, M. B.; Day, P. In *Advances in Inorganic Chemistry and Radiochemistry*; Emeléus, H. J., Sharpe, A. G., Eds.; Academic Press: San Diego, 1968; Vol. *10*, pp 247−422.
(39) Wilson, J. S.; Chawdhury, N.; Al-Mandhary, M. R. A.; Younus, M.; Khan, M. S.; Raithby, P. R.; Köhler, A.; Friend, R. H. *J. Am. Chem. Soc.* **2001**, *123*, 9412−9417.
(40) Silverman, E. E.; Cardolaccia, T.; Zhao, X.; Kim, K.-Y.; Haskins-Glusac, K.; Schanze, K. S. *Coord. Chem. Rev.* **2005**, *249*, 1491−1500.
(41) Prusakova, V.; McCusker, C. E.; Castellano, F. N. *Inorg. Chem.* **2012**, *51*, 8589−8598.
(42) Beljonne, D.; Wittmann, H. F.; Köhler, A.; Graham, S.; Younus, M.; Lewis, J.; Raithby, P. R.; Khan, M. S.; Friend, R. H.; Brédas, J. L. *J. Chem. Phys.* **1996**, *105*, 3868−3877.
(43) Muro, M. L.; Diring, S.; Wang, X.; Ziessel, R.; Castellano, F. N. *Inorg. Chem.* **2009**, *48*, 11533−11542.
(44) Whittle, C. E.; Weinstein, J. A.; George, M. W.; Schanze, K. S. *Inorg. Chem.* **2001**, *40*, 4053−4062.
(45) Archer, S.; Weinstein, J. A. *Coord. Chem. Rev.* **2012**, *256*, 2530−2561.
(46) Glik, E. A.; Kinayyigit, S.; Ronayne, K. L.; Towrie, M.; Sazanovich, I. V.; Weinstein, J. A.; Castellano, F. N. *Inorg. Chem.* **2008**, *47*, 6974−6983.
(47) Ramakrishna, G.; Goodson, T.; Rogers-Haley, J. E.; Cooper, T. M.; McLean, D. G.; Urbas, A. *J. Phys. Chem. C* **2009**, *113*, 1060−1066.
(48) Chen, W.-Z.; Fanwick, P. E.; Ren, T. *Organometallics* **2007**, *26*, 4115−4117.
(49) Chen, W.-Z.; Ren, T. *Inorg. Chem.* **2006**, *45*, 9175−9177.
(50) Xu, G.-L.; Ren, T. *Organometallics* **2005**, *24*, 2564−2566.
(51) Zhang, L.; Huang, Z.; Chen, W.-Z.; Negishi, E.; Fanwick, P. E.; Updegraff, J. B.; Protasiewicz, J. D.; Ren, T. *Organometallics* **2007**, *26*, 6526−6528.
(52) Iii, S. W. T.; Yagi, S.; Swager, T. M. *J. Mater. Chem.* **2005**, *15*, 2829−2835.
(53) Ren, T. *Organometallics* **2005**, *24*, 4854−4870.
(54) Ren, T. *Chem. Rev.* **2008**, *108*, 4185−4207.